

# CHEM**BIO**CHEM

## Supporting Information

### **Site-Specific Protein Labeling with Fluorophores as a Tool To Monitor Protein Turnover**

Yonatan G. Mideksa,<sup>[a]</sup> Maximilian Fottner,<sup>[a]</sup> Sebastian Braus,<sup>[a, c]</sup> Caroline A. M. Weiß,<sup>[a]</sup> Tuan-Anh Nguyen,<sup>[a]</sup> Susanne Meier,<sup>[a]</sup> Kathrin Lang,<sup>[a, b]</sup> and Matthias J. Feige<sup>\*[a, b]</sup>

cbic\_201900651\_sm\_miscellaneous\_information.pdf

## **Table of Contents**

- I. Methods**
- II. Supporting Figures**
- III. References**

## I. Methods

### General methods

All chemicals and solvents were obtained from commercial suppliers and used without further purification unless otherwise stated. Bicyclo[6.1.0]non-4-yn-9-ylmethanol (BCN) lysine (BCNK) was purchased from Synnifix and dissolved in 0.2 M NaOH, 15% DMSO (50 mM stock). Tetrazine-Amine AcOH salt was obtained from SiChem; Bodipy-TAMRA- and 5(6)-TAMRA-NHS ester fluorophore were obtained from Thermo Fisher Scientific. LC-MS was performed on an Agilent Technologies 1260 Infinity LC-MS system with a Phenomenex Aeris™ Peptide XB-C18 column (100 × 2.1 mm, 3.6 μm) for small molecules and a Phenomenex Jupiter C4 300 Å column (150 × 2 mm, 5 μm) for proteins, coupled to a 6310 Quadrupole spectrometer. The samples were analysed both in positive and negative mode followed by UV absorbance at 193, 254 and/or 280 nm. Reverse phase HPLC purification was carried out on a Shimadzu LC-20AT Prominence system with a Phenomenex Luna C18, 5 μm (4.6 × 250 mm) column. The solvent system consists of buffer A (MilliQ H<sub>2</sub>O +0.1% FA) and buffer B (MeCN +0.1% FA), which were used without filtration. Oligonucleotide primers were designed with NEBuilder and purchased from Sigma.

### Constructs

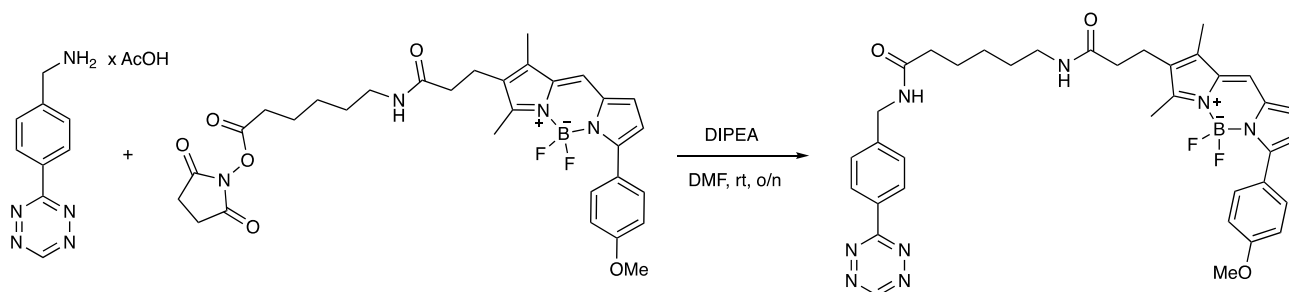
The plasmid bearing mCherry-TAG-GFP-HA/4× PyIT, sfGFP<sup>N150\*</sup>-His6/4× PyIT as well as the wt PylRS/4× PyIT vector that served as a basis for our new BCNKRS were described previously<sup>1</sup>. The mutations of BCNKRS1 (Y271G, C313V) were introduced in the wt PylRS/4× PyIT vector via site-directed mutagenesis. IL-12/23α inserts were generated through restriction-ligation subcloning in-frame downstream of the EF-1 promoter using NheI/NotI sites in place of mCherry-TAG-GFP-HA. Site-directed mutagenesis PCR using Pwo (Sigma-Aldrich) or Pfu (Promega) DNA polymerase replaced coding sequences in wild-type IL-12/23α with an amber codon (TAG). Reaction products were treated with DpnI prior to transformation. IL-12β was cloned into the pcDNA3.1(+) vector. All constructs were verified by sequencing. Hrd1 C291S-His<sub>6</sub> was described previously<sup>2, 3</sup>.

### Expression and purification of sfGFP<sup>N150\*</sup> using BCNKRS

Chemically competent *E. coli* K12 cells were co-transformed with pPyIT\_sfGFP<sup>N150\*</sup>-His6 (which encodes *MbtRNA*<sub>CUA</sub> and a C-terminally His6-tagged sfGFP gene with a TAG codon at position N150 under an arabinose-inducible promoter) and pBK\_BCNKRS or pBK\_wtRS

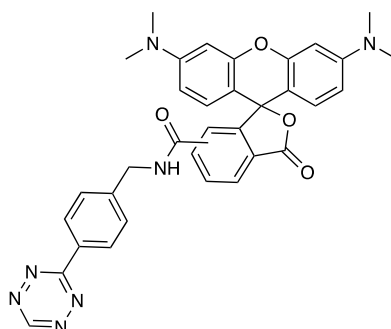
plasmids. After recovery with 1 mL SOC medium for one hour at 37 °C, cells were cultured overnight in 50 mL of non-inducing medium<sup>4</sup> containing full strength antibiotics (tetracycline and ampicillin), at 37°C, 200 rpm. The overnight culture was diluted to an OD<sub>600</sub> of 0.05 in auto-induction medium, supplemented with full-strength antibiotics (tetracycline and ampicillin) and 1 mM BCNK or 1 mM Bock. After overnight incubation at 37 °C, OD<sub>600</sub> was measured, 1 mL culture samples were harvested (4000 ×g, 15 min, 4 °C) and expression yields were analyzed by 15% SDS-PAGE with OD-normalized samples (100 µl 1× Laemmli per 1 OD unit; e.g. OD = 2.5 pellet of 1 mL culture was resuspended in 250 µl 1× Laemmli). sfGFP N150BCNK was purified as previously described<sup>5</sup>.

### Synthesis of Tetrazine-Bodipy-TMR conjugate



To a solution of tetrazine-amine AcOH salt (1.0 eq., 1.8 mg, 7.3 µmol) and fluorophore-NHS-ester (1.1 eq., 5 mg, 8.2 µmol) in dry DMF (3.5 mL), *N,N*-diisopropylethylamine (5.5 eq., 7 µL) was added and the reaction was stirred overnight at room temperature until LC-MS indicated reaction completion. The solvent was removed and the crude product was purified by preparative reverse phase HPLC to yield the final tetrazine-Bodipy-TAMRA conjugate (gradient: 25→90% B in buffer A) (LC-MS (m/z): calc. for C<sub>36</sub>H<sub>39</sub>BF<sub>2</sub>N<sub>8</sub>O<sub>3</sub> [M+Na]<sup>+</sup>: 703.6; detected: 703.3).

### Synthesis of Tetrazine-5(6)-TAMRA conjugate



The tetrazine-5(6)-TAMRA conjugate was synthesized and purified as described above for the Tetrazine-Bodipy-TMR conjugate using tetrazine-amine AcOH salt and 5(6)-TAMRA-NHS ester (LC-MS (m/z): calc. for  $C_{34}H_{29}N_7O_4$  [M+H]<sup>+</sup>: 600.2; detected: 600.2).

### Cell Culture and Transient Transfections

HEK-293T cells were grown in Dulbecco's modified Eagle's medium (DMEM) containing L-Ala-L-Gln (AQmedia, Sigma-Aldrich) supplemented with 10% (v/v) fetal bovine serum (Biochrom) and 1% (v/v) antibiotic-antimycotic solution (25 µg/mL amphotenicin B, 10 mg/ml streptomycin, and 10,000 units of penicillin; Sigma-Aldrich) at 37°C and 5% CO<sub>2</sub>. Transfections were performed using GeneCellin (BioCellChallenge) or Torpedo (Ibidi) according to manufacturers' instructions. Cells were transfected in poly-D-lysine coated 35mm dishes (Corning) with 1 µg of IL-12/23α/sfGFP<sup>N150\*</sup> constructs and 1 µg BCNK-RS/PyIT for all expression and pulse/chase experiments. To analyze attenuation of protein degradation using E3 activity-defective mutant of Hrd1, 0.75 µg α-subunit, 0.75 µg BCNK-RS/PyIT and 0.5 µg empty vector or Hrd1 C291S - His<sub>6</sub> was transfected to cells in the presence of complete DMEM with BCNK. For wt IL-12α BCNK-RS/PyIT was not included in the CHX assay to assess the effect of Hrd1. Samples were collected for subsequent analysis 24 – 48 h post-transfection. 2 µg of total DNA in a 1:1:2 ratio (α-subunit:BCNK-RS/PyIT:12β) was transfected for *in cellulo* secretion and assembly tests, which were performed as described in<sup>6,7</sup>, except for supplementing fresh complete DMEM with BCNK directly before and for 8 h after transfection (to obtain secretion samples). Cells were washed in PBS and lysed in RIPA lysis buffer (50mM Tris/HCl pH 7.5, 150mM NaCl, 1% NP40, 0.1% SDS, 0.5% DOC, 1× Roche complete protease inhibitor w/o EDTA; Roche Applied Science) supplemented with 20 mM N-ethylmaleimide (NEM, Sigma-Aldrich).

Where indicated, 24 h post-transfection cells were chased with either 50 µg/mL cycloheximide solution (Sigma-Aldrich) or 1 mM BCNK after 4-5 washing steps and 15 min labeling with either Bodipy TMR-tetrazine or SiR-tetrazine, using complete DMEM in a humidified environment at 37°C and 5% CO<sub>2</sub>, for the indicated time points (0 h: untreated). Protein remaining was calculated as a percentage of untreated, and linear regression fittings on semi-log curves were used to calculate protein half-lives. Where indicated, cells were treated with 10 µM MG132 (Sigma-Aldrich) for 3 h (including time required for the washing steps) prior to the *uChase* assay followed by co-incubation with BCNK.

### **Site-specific unnatural amino acid incorporation and Biorthogonal Labeling**

HEK-293T cells were transiently transfected with the indicated constructs in the presence or absence of bicyclo[6.1.0]nonyne-lysine (BCNK) at different concentrations in complete DMEM. Before labeling, after 24 – 48 h expression, BCNK containing growth medium was removed and cells were repeatedly washed with pre-warmed fresh medium at intervals of 20 min over 2 h to wash out excess BCNK whilst incubation in a humidified atmosphere with 5% CO<sub>2</sub> at 37°C was continued in between. TAMRA-tetrazine (see above), Bodipy TMR-tetrazine (see above) or SiR-tetrazine (SC-008, Spirochrome) conjugates in complete DMEM (each at 2mM stock concentration) were then added to cells incubated for the specified times in a humidified atmosphere with 5% CO<sub>2</sub> and 37°C.

For labeling of secreted proteins to be used in iLite™ assays, medium samples were treated with 2 µM SiR-tetrazine for 1 hour at 37°C with gentle mixing after supplementation with 10× RIPA w/o detergents (500 mM Tris/HCl pH 7.5, 1.5 M NaCl, 10× Roche complete protease inhibitor w/o EDTA; Roche Applied Science).

### **Immunoprecipitation and immunoblotting experiments**

Whole cell lysate samples were immunoprecipitated overnight with anti-IL-12 $\alpha$  (1:240 (v/v), abcam ab133751) antibody. Immunocomplexes were isolated with Protein A/G agarose beads (Santa Cruz Biotechnology, USA, sc-2003) for 1 h under rotation at 4°C and eluted with 2× Laemmli buffer with 10% (v/v)  $\beta$ -mercaptoethanol after washing three times with 1 ml RIPA lysis buffer.

Inputs (1, 2 or 4%) and immunoprecipitated cell lysates (72%) were supplemented with Laemmli and boiled at 95°C for 5 min and then separated on SDS-polyacrylamide gels and transferred to a PVDF membrane (Biorad, USA). After blocking for 12 – 24 h (at RT or 4°C) with MTBST (25 mM Tris/HCl pH 7.5, 150 mM NaCl, 5% skim milk powder, 0.05% Tween) or gelatin buffer (0.1% gelatin, 15 mM Tris/HCl pH 7.5, 130 mM NaCl, 1mM EDTA, 0.1% Triton X-100) proteins of interest were detected using anti-IL-12 $\alpha$  (abcam ab133751, 1:1000 in MTBST), anti-IL-23 $\alpha$  (Biolegend #511202, 1:500 in MTBST), anti-IL-12 $\beta$  (abcam ab133752, 1:500 in MTBST), anti-His<sub>6</sub> conjugated to HRP (Sigma-Aldrich 11965085001, 1:2000 in MTBST) or anti-Hsc70 (Santa Cruz sc-1059, 1:1000 in gelatin buffer). HRP-coupled donkey anti-goat (Santa Cruz sc-2020/sc-2354), goat anti-mouse (sc-2031), mouse-IgG $\kappa$  BP (Santa Cruz sc-516102), or goat anti-rabbit (Santa Cruz sc-2054/sc-2357) secondary antibodies/binding proteins were used for immunoblot analyses. Blots were detected using ECL prime (Amersham) on a Fusion Pulse 6 imager (Vilber Lourmat).

## In-gel fluorescence assays

In-gel fluorescence was visualized on a Typhoon™ Variable Mode Imager 9200 (GE Life Sciences). A green (532 nm) excitation laser and a 580 nm / 30 nm bandpass emission filter was used for TAMRA or B-TMR, whereas a red (633 nm) excitation Laser and a 670 nm / 30 nm bandpass emission filter was used for detecting SiR.

## Receptor binding assays

To verify if the secreted IL-12/23 can elicit appropriate biological responses in terms of their distinct receptor binding, we used the iLite™ (Euro Diagnostica) cell-based reporter assay in the presence or absence of SiR-tetrazine. 40 µL of cell culture supernatant containing secreted IL-12 or IL-23 were added to sterile white F-bottom shaped 96-well plates (BRANDplates®, BRAND GmbH) and incubated with 40 µL iLite™ IL-12/23 Assay Ready Cells (Euro Diagnostica) for 5 hours at 37°C, 5% CO<sub>2</sub>. For initiation of luminescence, cells were incubated with the Dual-Glo® Luciferase Assay System (Promega) and the signals of Firefly (proportional to the functional activity of IL-12/23) and Renilla Luciferase (housekeeping signal) were detected with a microplate luminometer (Tecan Spark). Individual signals were normalized against the housekeeping renilla signal. To allow better comparisons between mutants, the highest receptor activation signal was always set to 1. Comparable secretion levels were confirmed by immunoblots.

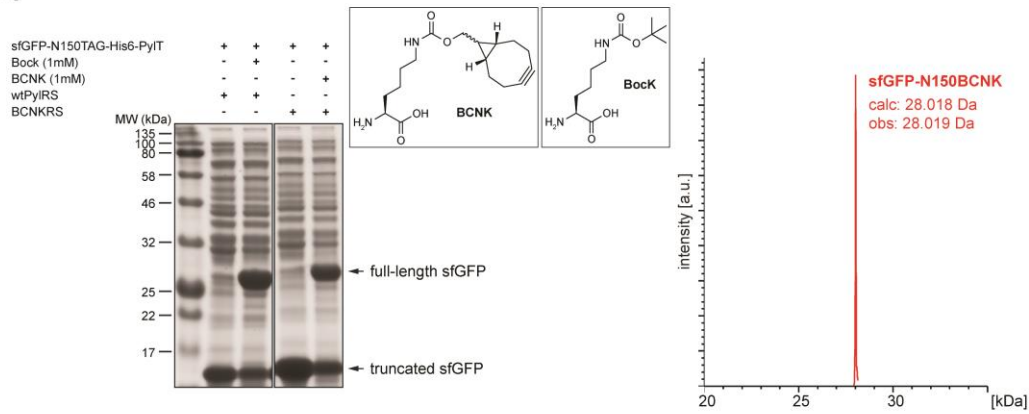
## Software and Statistics

Missing loops in the IL-12 and IL-23 structures were modelled *in silico* with YASARA Structure (www.yasara.org) and the final structure was energy minimized. Sites for BCNK incorporation were selected based on residue solvent accessibility (PDBePISA server<sup>8</sup>) and mutation stability prediction (SDM server<sup>9</sup>) calculated using available crystal structure data (PDB codes: 3HMX, 1F45, 3DUH, 5MXA and 5MZV). Protein structures were visualized with PyMOL. Western blot and in-gel fluorescence raw images were processed for brightness and contrast in ImageJ. Statistical analyses and graph fittings were performed with Prism 7 (GraphPad) software. The relative labeling signal-to-noise ratio in SI Figure 3D was obtained by applying the following formula to the in-gel fluorescence band intensities (upper/lower background: all signal above/below the IL-12α D31BCNK or sfGFP N150BCNK band):

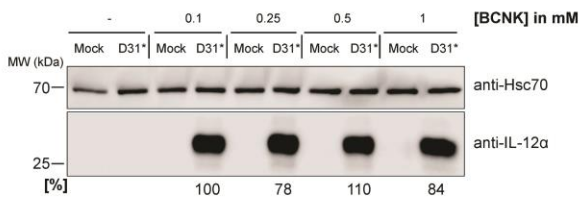
$$\text{Relative labeling S/N} = \frac{I_{\text{IL-12}\alpha \text{ D31BCNK}} / (I_{\text{upper background}} + I_{\text{lower background}})_{\text{IL-12}\alpha \text{ D31BCNK}}}{I_{\text{sfGFP N150BCNK}} / (I_{\text{upper background}} + I_{\text{lower background}})_{\text{sfGFP N150BCNK}}}$$

## II. Supporting Figures

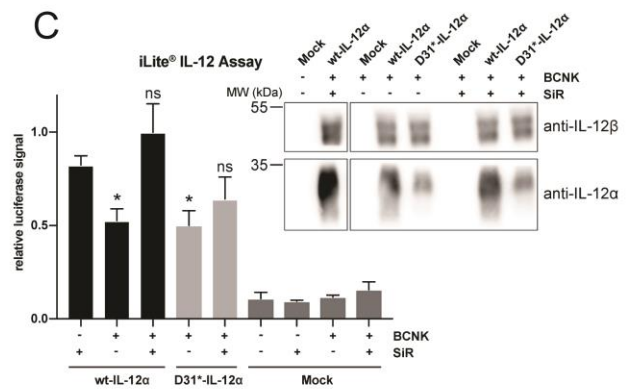
A



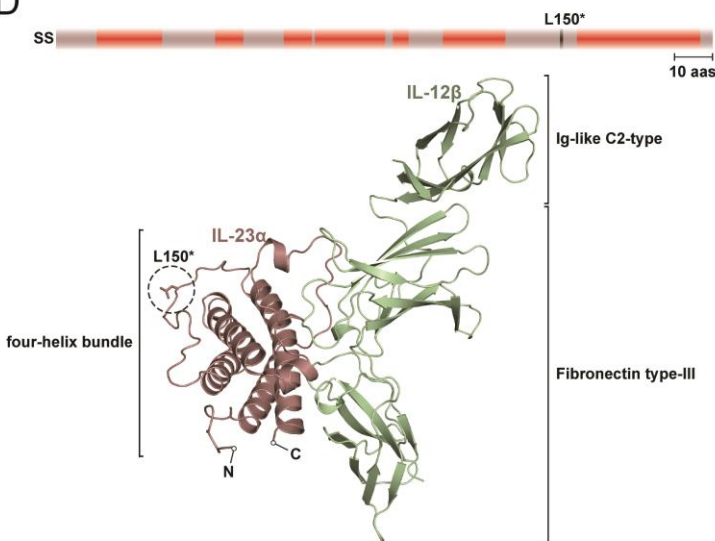
B



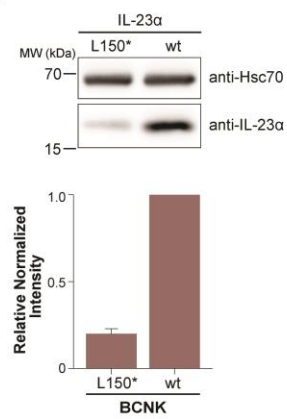
C



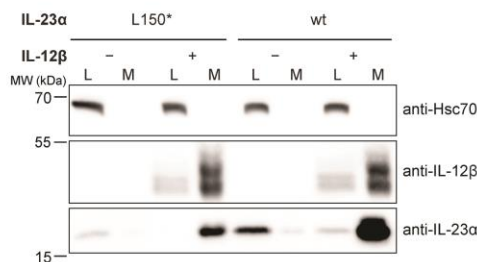
D



E



F



G

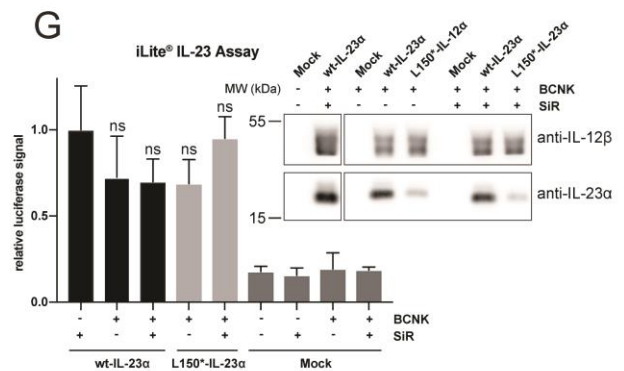




**Figure S1. Site-specific incorporation of BCNK into proteins and characterization of BCNK-modified IL-12 and IL-23.**

A) Site-specific incorporation of BCNK into sfGFP-150TAG-His6 using BCNKRS. Test expressions in *E. coli* show that BCNK incorporation is nearly as efficient as BockK incorporation. Full-length ESI-MS confirms selective incorporation of BCNK.

B) HEK-293T cells expressing the BCNKRS/PyIT pair and IL-12 $\alpha$  D31\* were assayed in the presence of increasing amounts of BCNK. Numbers below immunoblots are relative quantifications of expression levels (0.1 mM BCNK set to 100%).

C) iLite™ assay to test biological functionality of secreted wild-type IL-12 versus IL-12 containing IL-12 $\alpha$  D31BCNK in the presence of BCNK and fluorophore where indicated. Normalized results of Firefly/Renilla Luciferase signal are displayed together with immunoblots of medium samples (N=3 for 'wt' and 'Mock', N=6 for 'TAG variants', mean $\pm$ SEM, \**p-value* < 0.05, ns: not significant; comparison always refer to wt + SiR). Note that concentrations of the interleukins in the media were not determined and may be above the linear range of the assay, so that only qualitative conclusions should be drawn from the activity tests.

D) (Top) Schematic representation of IL-23 $\alpha$  secondary structure as in Figure 1A. (Bottom) PDB structure of heterodimeric IL-23 (PDB code: 3DUH, missing residues were modelled), N- and C-terminus are indicated for IL-23 $\alpha$ . The position selected for UAA incorporation into IL-23 $\alpha$  is marked with a dashed circle.

E) (Top) Representative immunoblot of HEK-293T cells expressing the BCNK-RS/PyIT pair and IL-23 $\alpha$  L150TAG (abbreviated as L150\*) in the presence of BCNK. (Bottom) Quantification of IL-23 $\alpha$  L150BCNK expression relative to wild-type expression was quantified by immunoblots, N=3 (mean $\pm$ SEM).

F) BCNK-modified IL-23 $\alpha$  L150\* was tested for assembly-induced secretion upon co-expression of IL-12 $\beta$  (analogous to Figure 1, C and D). L: Lysate; M: Medium; wt: wild-type control.

G) Same as in (C) for IL-23 $\alpha$  L150BCNK.

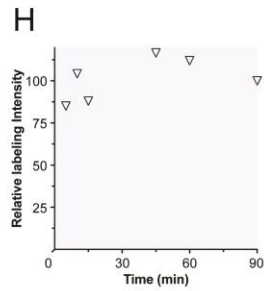
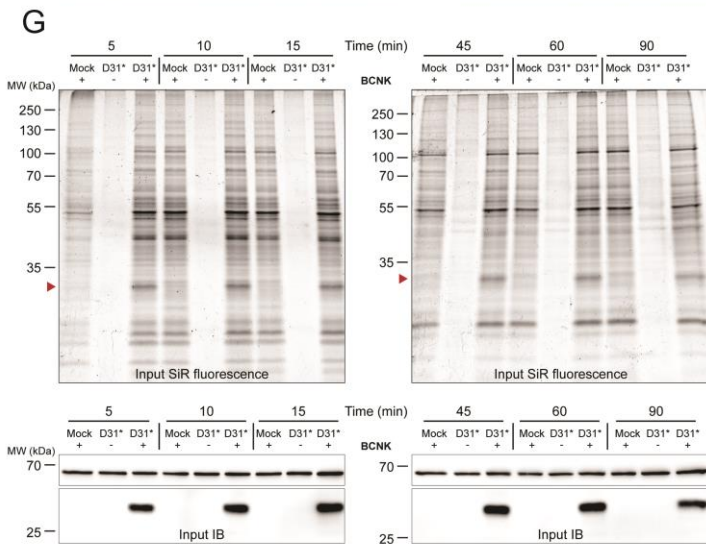
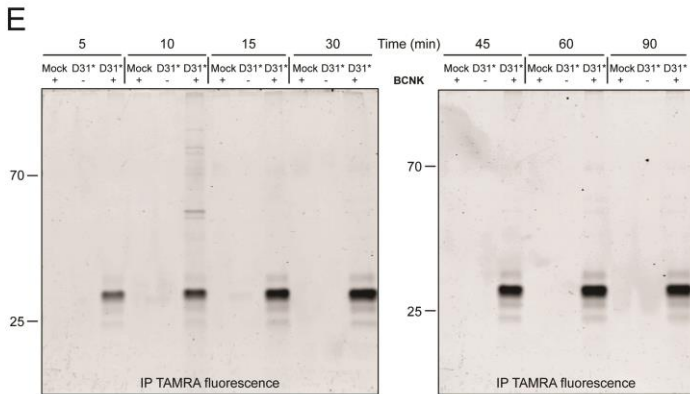
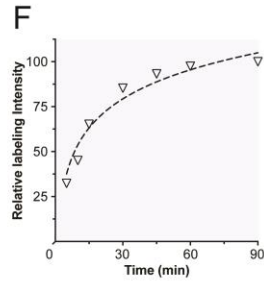
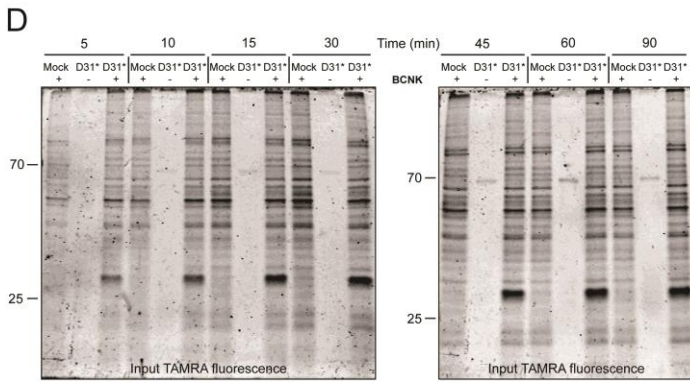
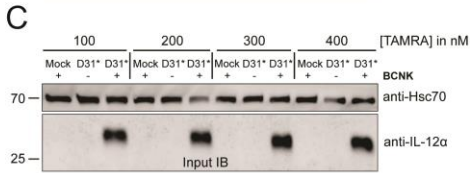
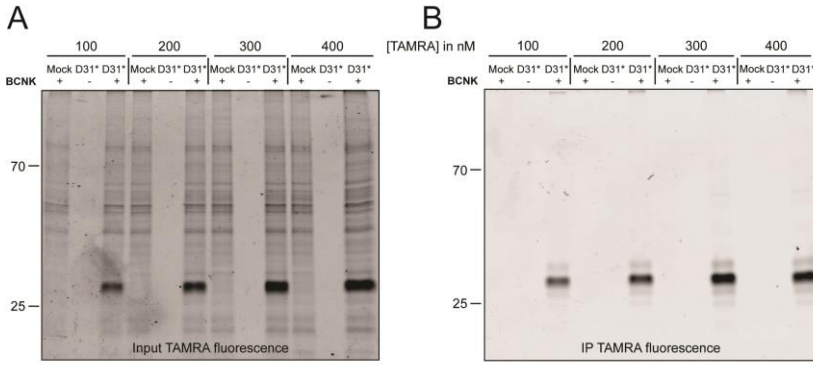


**Figure S2. Bio-orthogonal labeling degree and efficiency of BCNK-modified IL-12 $\alpha$ .**

A-C) Cells expressing empty vector (mock) or IL-12 $\alpha$  D31\* at 0.25 mM BCNK were treated with the indicated concentrations of TAMRA-tetrazine fluorophore and analyzed by in-gel fluorescence of lysates (A), after immunoprecipitation (IP) (B), as well as by immunoblotting (C).

D-F) TAMRA-tetrazine labeling of lysates after different time points (D) and after additional immunoprecipitation (IP) (E) at intervals ranging from 5 – 90 min were analyzed using in-gel fluorescence. (F) Quantification of relative labeling from lysates with 90 min set to 100 with non-linear (exponential) graph fitting.

G, H) (G) Same as in (D) with 400 nM SiR-tetrazine labeling of lysates including immunoblotting (*bottom panel*). (H) Quantification of relative labeling as in (F).

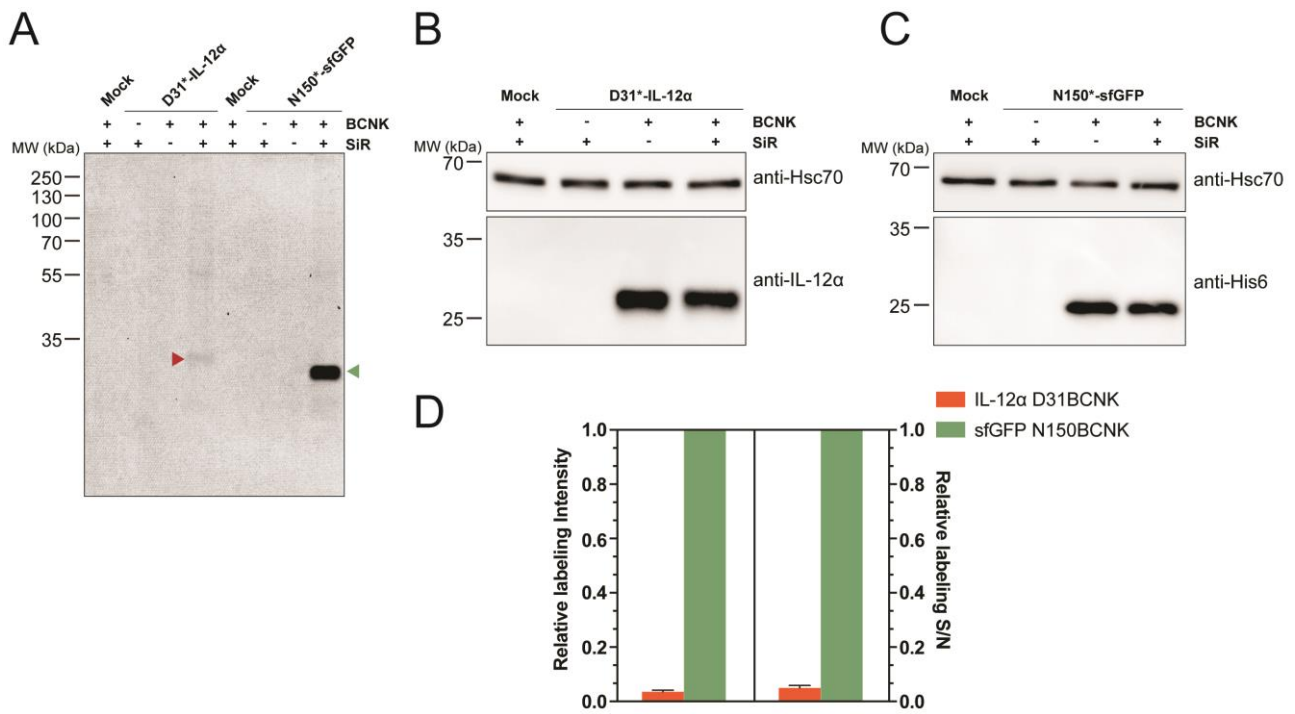


**Figure S3. Comparison of background labeling for BCNK-modified IL-12 $\alpha$  versus sfGFP in mammalian cells.**

A) In-gel fluorescence of HEK-293T cells expressing the indicated constructs in the presence (+) or absence (-) of 0.25 mM BCNK and/or 400 nM SiR-tetrazine fluorophore. Red and green arrows show the position of labeled IL-12 $\alpha$  D31BCNK and sfGFP N150BCNK, respectively.

B, C) Representative immunoblots of samples in (A) with Hsc70 as a loading control.

D) Quantifications of relative labeling intensity and signal-to-noise ratio (levels for sfGFP N150BCNK were set to 1). Measurements were taken from N=6 in-gel fluorescence datasets of lysates (mean $\pm$ SEM).

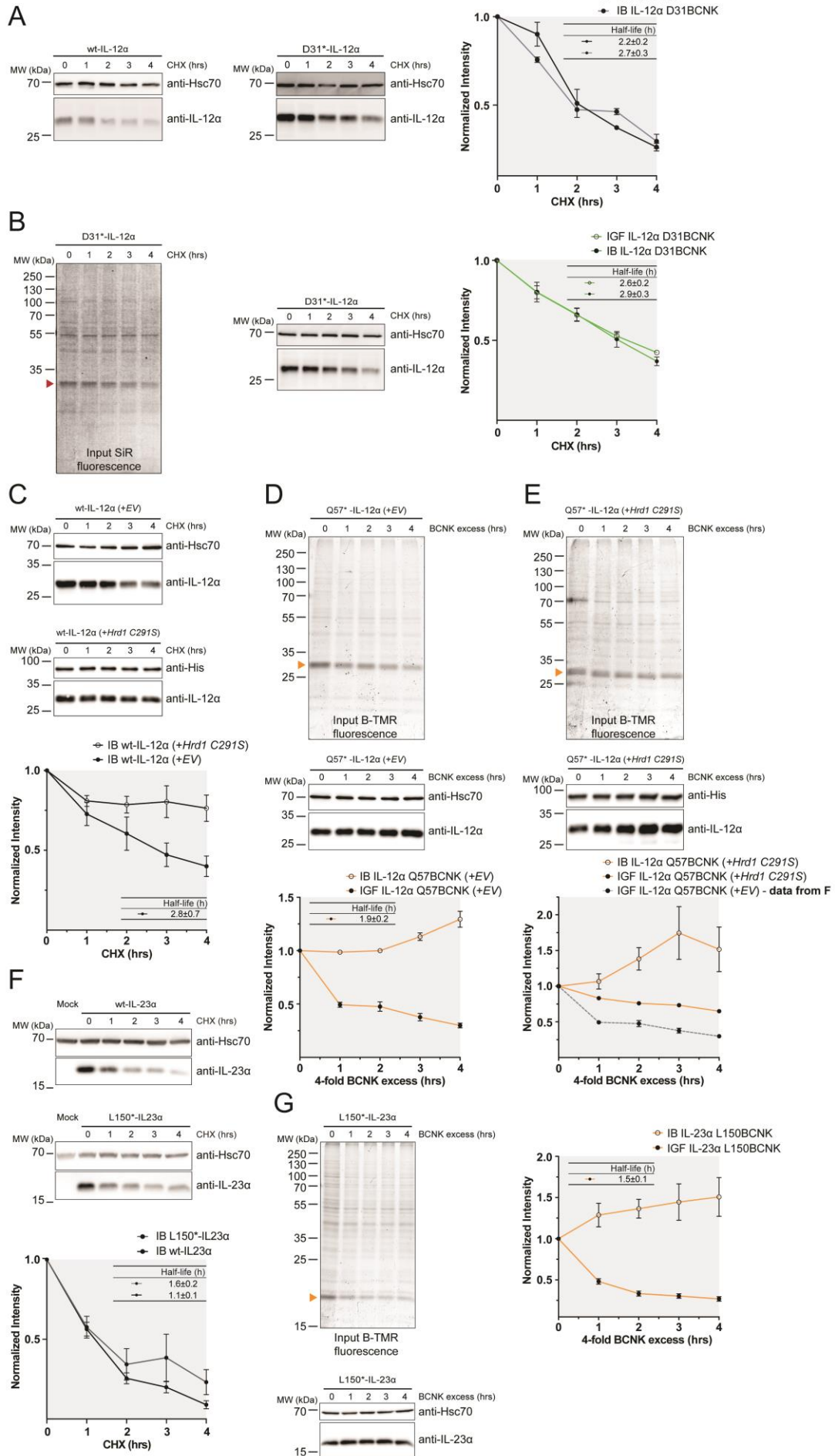


**Figure S4. *uChase* protein turnover assay benchmarked using Cycloheximide chase assays and extended to monitor degradation of IL-23 $\alpha$ .**

A) Representative immunoblots to follow degradation of wild-type IL-12 $\alpha$  versus IL-12 $\alpha$  D31BCNK in the presence of BCNK using Cycloheximide for the indicated times (0 – 4 hr). Quantifications of the data from N=3 for wt/D31BCNK (mean $\pm$ SEM) are shown on the right.

B) CHX-chase for SiR-labeled IL-12 $\alpha$  D31BCNK. A representative in-gel fluorescence and immunoblot is shown together with quantification from N=3 biological replicates (mean $\pm$ SEM).

C) CHX-chase representative immunoblots to follow turnover of wild-type IL-12 $\alpha$  in the presence of BCNK upon overexpression of mock or inactive Hrd1 C291S - His<sub>6</sub> mutant. Quantification of the data from N=3 (mean $\pm$ SEM – *bottom panel*).

D, E) The effect of overexpression of Hrd1 C291S - His<sub>6</sub> mutant on IL-12 $\alpha$  Q57BCNK degradation (G) was analyzed using the *uChase* assay compared to a mock control (F). (Bottom) The graphs show quantifications from in-gel fluorescence and immunoblots, N=3 (mean $\pm$ SEM). A reference trace (G – *bottom panel*, dotted grey line) shows the same data as obtained by the in-gel fluorescence in (F – *bottom panel*).

F) The same as in (A) but for IL-23 $\alpha$  L150BCNK (N=5, (mean $\pm$ SEM)).

G) *uChase* assay as in Figure 3, C and D but for IL-23 $\alpha$  L150BCNK labeled with B-TMR. Quantification of the data (*right panel*) from N=6 in-gel fluorescence and immunoblot datasets of lysates (mean $\pm$ SEM). The slight increase in immunoblots can likely be attributed to the fact that first, UAAs are washed out, possibly causing some degradation of IL-23 $\alpha$  L150BCNK during the phase of UAA-absence, and then an excess of UAA is added, leading to resumed translation. It can be expected that this effect depends on the protein's half-life and is thus more pronounced for IL-23 $\alpha$  versus IL-12 $\alpha$ .

### III. References

1. Schmied, W. H.; Elsasser, S. J.; Uttamapinant, C.; Chin, J. W., Efficient multisite unnatural amino acid incorporation in mammalian cells via optimized pyrrolysyl tRNA synthetase/tRNA expression and engineered eRF1. *J Am Chem Soc* **2014**, *136* (44), 15577-83.
2. Coelho, J. P. L.; Stahl, M.; Bloemeke, N.; Meighen-Berger, K.; Alvira, C. P.; Zhang, Z. R.; Sieber, S. A.; Feige, M. J., A network of chaperones prevents and detects failures in membrane protein lipid bilayer integration. *Nature communications* **2019**, *10* (1), 672.
3. Nadav, E.; Shmueli, A.; Barr, H.; Gonen, H.; Ciechanover, A.; Reiss, Y., A novel mammalian endoplasmic reticulum ubiquitin ligase homologous to the yeast Hrd1. *Biochem Biophys Res Commun* **2003**, *303* (1), 91-7.
4. Hammill, J. T.; Miyake-Stoner, S.; Hazen, J. L.; Jackson, J. C.; Mehl, R. A., Preparation of site-specifically labeled fluorinated proteins for <sup>19</sup>F-NMR structural characterization. *Nature protocols* **2007**, *2* (10), 2601-7.
5. Fottner, M.; Brunner, A.-D.; Bittl, V.; Horn-Ghetko, D.; Jussupow, A.; Kaila, V. R. I.; Bremm, A.; Lang, K., Site-specific ubiquitylation and SUMOylation using genetic-code expansion and sortase. *Nature chemical biology* **2019**, *15* (3), 276-284.
6. Reitberger, S.; Haimerl, P.; Aschenbrenner, I.; Esser-von Bieren, J.; Feige, M. J., Assembly-induced folding regulates interleukin 12 biogenesis and secretion. *J Biol Chem* **2017**, *292* (19), 8073-8081.
7. Muller, S. I.; Friedl, A.; Aschenbrenner, I.; Esser-von Bieren, J.; Zacharias, M.; Devergne, O.; Feige, M. J., A folding switch regulates interleukin 27 biogenesis and secretion of its alpha-subunit as a cytokine. *Proceedings of the National Academy of Sciences of the United States of America* **2019**, *116* (5), 1585-1590.
8. Krissinel, E.; Henrick, K., Inference of macromolecular assemblies from crystalline state. *J Mol Biol* **2007**, *372* (3), 774-97.
9. Pandurangan, A. P.; Ochoa-Montano, B.; Ascher, D. B.; Blundell, T. L., SDM: a server for predicting effects of mutations on protein stability. *Nucleic acids research* **2017**, *45* (W1), W229-w235.